JOURNAL OF GEOPHYSICAL RESEARCH, VOL. 103, NO. A2, PAGES 2359–2368, FEBRUARY 1, 1998

Hydromagnetic wave propagation and coupling in a magnetotail waveguide

W. Allan

National Institute of Water and Atmospheric Research, Wellington, New Zealand

Andrew N. Wright

Mathematical Institute, University of St. Andrews, St. Andrews, Scotland

Abstract. For some time the magnetotail has been considered as a possible region where hydromagnetic waves can propagate as waveguide modes. Recently, attention has turned to the magnetospheric flanks as waveguides, and much useful insight has been gained into propagation of fast waveguide modes there, and the structure of the field line resonances they can drive. We return to the magnetotail and investigate hydromagnetic wave propagation and coupling in a magnetotail waveguide. This problem is significantly different from the flank waveguide as the ambient magnetic field is directed along the waveguide rather than across. Field line resonances of the flank type are not possible in the lobe waveguide. We describe a numerical simulation of a model waveguide in which the Alfvén speed decreases across the waveguide to the central plasma sheet. The waveguide is stimulated by a short compressional perturbation located in the far tail. The cross-tail spatial structure is chosen to give relatively weak coupling between fast and Alfvén modes so that phase and group velocities of uncoupled fast modes can be used to interpret the results. We find that the perturbation propagates dispersively down the waveguide in the form of fast waveguide modes. Fourier components with small parallel wavenumber contain most of the energy, and propagate relatively slowly toward the "Earth." These act as moving sources which launch Alfvén waves continuously earthward. The wave dispersion relations are such that the waveguide modes couple with Alfvén waves only in a limited region of the transverse Alfvén speed gradient. The Alfvén waves travel at the local Alfvén speed along each field line, so that as they travel the wave on a given field line becomes increasingly out of phase with waves on adjacent field lines. The phase mixing in our model is novel in that it includes the effects of transverse gradients in both Alfvén frequency and parallel wavenumber which tend to cancel each other out. Nevertheless, the phase-mixing process leads to increasingly fine transverse structure as the waves progress down the waveguide. The results are likely to be applicable in regions such as the plasma sheet boundary layer and the plasma mantle.

1. Introduction

The existence of an extended geomagnetic tail has been appreciated for more than three decades. Relatively early in that period it was also appreciated that the large size of this cavity might allow the existence of hydromagnetic eigenmodes with millihertz and submillihertz frequencies, as an explanation for the observation of such frequencies in magnetometer data [e.g., *Herron,* 1967]. The "theta" model used by *McClay and Radoski* [1967] derived reasonable eigenfrequencies from a cylindrical magnetotail with uniform antiparallel magnetic fields in the top and bottom halves of the cylinder, and a uniform Alfvén speed. The cylinder was bounded by reflecting walls perpendicular to the axis. Similar results were obtained by *Patel* [1968]. Recently, *Walker et al.* [1993] have again considered waveguide eigenfrequencies in a cylindrical magnetotail.

Increasingly detailed models were developed to include the plasma sheet [*Siscoe,* 1969] and solar wind flow coupling to the plasma sheet via hydromagnetic waves [*McKenzie,* 1970, 1971]. Work on waves related to the plasma sheet and neutral sheet has been sporadic since then [*Hopcraft and Smith,* 1986; *Seboldt,* 1990; *Liu et al.,* 1995], although much related work has been carried out in modeling the solar at-

Paper number 97JA02874.
0148-0227/98/97JA-02874$09.00

mosphere [e.g., *Roberts et al.*, 1984; *Berghmans et al.*, 1996], with some application of the results to the magnetosphere [*Edwin et al.*, 1986].

Waveguide ideas have recently come to the fore as an explanation for certain very stable, discrete field line resonance signatures seen in high-frequency radar observations of the ionosphere [*Samson et al.*, 1992; *Walker et al.*, 1992]. The waveguides were proposed to lie on the magnetospheric flanks so that magnetic field lines were transverse rather than longitudinal as in the tail case. Fast waveguide modes could then drive field-line resonances on these field lines which were line-tied in the ionosphere. Detailed time-dependent results for flank waveguide modes and field line resonances were derived by *Wright* [1994], *Rickard and Wright* [1994, 1995], and *Wright and Rickard* [1995].

Recent observations have returned attention to the magnetotail as a possible hydromagnetic waveguide. *Elphinstone et al.* [1995] presented IMP 8 observations of compressional waves in the northern tail lobe, which appeared to be propagating Earthward from a source tailward of $x_{GSE} = -28\,R_E$. *Weatherwax et al.* [1997] discussed observations of Pc5 pulsations with frequencies of a few millihertz on high-latitude field lines which mapped deep into the tail, but which were probably still closed. *Ables et al.* [1996] and *Wolfe et al.* [1997a, b] presented ground-based magnetometer observations of mHz frequency ULF waves in the southern polar cap, which should map to open field lines in the southern magnetotail lobe. These observations all indicate the occurrence of wave activity on field lines which extend well into the region where the magnetotail should act as a hydromagnetic waveguide. Note that *Wolfe et al.* [1997a] effectively summarized the results of *Wolfe et al.* [1997b], which are similar to the results of *Ables et al.* [1996].

Our intention in this paper is to develop a numerical simulation of hydromagnetic wave propagation and coupling in a simplified model of the magnetotail. This initial work is aimed at determining qualitative features of these processes and hence identifying the fundamental physical processes that operate. A detailed observational comparison will be carried out in later work. Therefore we do not at present attempt to compare our results directly with the observations described above.

We retain full time dependence rather than examining tail eigenmodes as was generally done in the earlier magnetotail work cited above. We regard coupling between compressional fast waves and Alfvén waves as being important, and therefore include appropriate Alfvén speed gradients and cross-tail spatial structure to allow this coupling. Note that the simple cross-tail structure used here is not intended to be a realistic model of the magnetotail, but should be regarded as a demonstration of the physical effects that can occur in any region of the magnetotail where significant cross-tail Alfvén speed gradients occur.

In the following sections we describe the model structure, the numerical simulation, and the results. Finally, we interpret the physical meaning of the results and discuss their applicability to the magnetosphere.

2. Model Structure

Our model magnetotail waveguide is based on the two-dimensional hydromagnetic box model of *Radoski* [1971] and *Southwood* [1974]. The main difference between the present case and the flank waveguide model of *Rickard and Wright* [1994] (hereinafter RW) is that the magnetic field extends parallel to the waveguide axis rather than being across the waveguide as in the latter work. Figure 1 is a schematic of the waveguide. The coordinate x extends from a position in the tail at $x = 0$ to $x = x_E$, the "Earth." The coordinate z extends across the waveguide from $z = -z_M$ at the southern "magnetopause" to $z = z_M$ at the northern "magnetopause." Note that in this qualitative model $z = \pm z_M$ need not necessarily be taken as representing the magnetopause in the physical magnetotail but are convenient boundaries for the region of cross-tail Alfvén speed variation described below. Variation in the third dimension y is represented by a single Fourier component as described later.

The magnetic field $\mathbf{B} = B_0\hat{\mathbf{x}}$ is uniform. Plasma mass density is chosen to vary as a function of z in such a way that the Alfvén speed V_A varies linearly across the northern and southern "lobes" as shown in Figure 1.

$$V_A(z) = \frac{1}{2}\left(1 + \frac{|z|}{z_M}\right) \tag{1}$$

V_A changes by a factor of 2 between $z = 0$ and $z = \pm z_M$. We have in effect assumed a very thin plasma sheet at $z = 0$ with no neutral line so that we can use a magnetic field of constant strength that reverses direction across $z = 0$ (as in the cylindrical model of *McClay and Radoski* [1967]). This is fairly unrealistic but is adequate for modeling the propagation of hydromagnetic waves in a cold plasma, as this propagation depends only on V_A rather than the magnetic field and density independently and does not depend on the direction of $\mathbf{B}$. The linear variation of V_A is also a major simplification. This variation is chosen for numerical convenience, in order to ensure that the Alfvén wave phase-mixing length (see RW)

$$L_{PH}(z,t) = 2\pi[\omega_A'(z)t]^{-1} \tag{2}$$

is constant across each "lobe" of the model magnetotail at a given time. Here $\omega_A(z)$ is the frequency of an

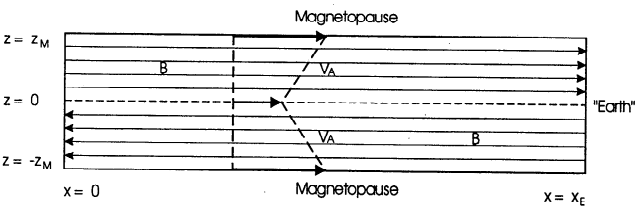

Figure 1. Schematic of the model waveguide, showing the variation of the Alfvén speed V_A between the "plasma sheet" (horizontal dashed line) and the nominal "magnetopause." The constant magnitude magnetic field $\mathbf{B}$ reverses direction across the "plasma sheet." The y direction is into the plane of the diagram.

Alfvén wave witha given wavelength on the field line at z, the prime denotes d/dz and t is elapsed time. Constant L_{PH} at a given time ensures that a grid spacing in the numerical scheme which resolves L_{PH} at one z resolves it at all z in the lobe. Even with this idealized variation of V_A, we expect that our results should be at least qualitatively applicable to regions where there is a transverse variation of the Alfvén speed in the physical magnetosphere. Later (in section 5.2) we show (2) is actually an underestimate of the rather subtle phase-mixing length which occurs in our model.

We solve the following set of linearized first-order ideal hydromagnetic equations in the waveguide.

$$\partial b_x/\partial t = -(\partial u_z/\partial z + k_y u_y) \quad (3)$$

$$\partial b_y/\partial t = \partial u_y/\partial x \quad (4)$$

$$\partial b_z/\partial t = \partial u_z/\partial x \quad (5)$$

$$\partial u_y/\partial t = (\partial b_y/\partial x + k_y b_x)/\rho \quad (6)$$

$$\partial u_z/\partial t = (\partial b_z/\partial x - \partial b_x/\partial z)/\rho \quad (7)$$

Here $\mathbf{b} = (b_x, b_y, b_z)$ is the wave magnetic field, $\mathbf{u} = (0, u_y, u_z)$ is the wave $\mathbf{E} \times \mathbf{B}$ drift velocity, and ρ is the plasma mass density. The velocity u_y is chosen to have a separable y variation of $\sin(k_y y)$, with $u_y = 0$ at the y boundaries of the waveguide. The other field components have y variations consistent with this.

These hydromagnetic equations have been normalized using z_M as the unit of distance, and z_M/V_{AM} as the unit of time, where V_{AM} is the Alfvén speed at $z = \pm z_M$. Velocities are normalized using V_{AM}, magnetic fields using B_0, and densities using $B_0^2/\mu_0 V_{AM}^2$. From now on all quantities quoted will be normalized.

Boundaries are chosen to be perfectly reflecting at the "magnetopause" ($u_z(z = \pm z_M) = 0$) and at the "earthward" end of the box ($x = x_E$), the latter crudely representing the high-latitude ionosphere. (Note that the simulation was not run long enough for waves to reach the Earthward end of the computational domain, so this boundary does not affect the results.) Symmetry boundary conditions are applied at the $x = 0$ end of the waveguide ($\partial u_z/\partial x = 0$).

Waves in the guide are stimulated by a compressional disturbance in u_z occurring along the "plasma sheet" $z = 0$ over the range $x = 0$ to x_d (where x_d is short compared with x_E) and for a time t_d short compared with the minimum Alfvén transit time to x_E. The form of the disturbance is

$$u_z \propto \cos(\pi t/t_d)[1 - \cos(2\pi t/t_d)][1 + \cos(\pi x/x_d)] \quad (8)$$

for $t \leq t_d$, with $u_z = 0$ for $t > t_d$. This imposed velocity at $z = 0$ corresponds to a positive displacement at $z = 0^+$, and a negative displacement at $z = 0^-$. The associated expansion of the field lines in the z direction could arise from a flux rope or plasmoid moving down the tail. This disturbance can be thought of as representing a sudden localized energy release in the tail plasma sheet.

Wright [1994] and RW discussed the dispersive propagation of fast mode waves in inhomogeneous hydromagnetic waveguides. They showed that the phase and group velocity properties of the uncoupled ($k_y = 0$) WKB solutions were useful for interpretation of the coupled wave results. Here we give these properties for the tail waveguide using the appropriate dispersion and group velocity diagrams. In the top panel of Figure 2 the full curve shows the waveguide mode parallel dispersion relation (frequency ω versus $k_\parallel = k_x$) for the fundamental $n = 1$ mode in z when $k_y = 0$. This curve was calculated using a shooting method, with boundary conditions $u_z = 0$ at $z = \pm 1$. A mode with wavenumber $k_\parallel$ has a parallel phase velocity given by $V_{p\parallel} = \omega/k_\parallel$. The dashed lines show Alfvén wave dispersion relations for the range of V_A in the model, from $V_A = 0.5$ at $z = 0$ to $V_A = 1$ at $z = 1$, including $V_A = 0.9$ at $z = 0.8$. The dash-dot line shows in arbitrary units the $k_\parallel$ Fourier amplitude spectrum of the applied impulse (8) for $x_d = 1.2$. The full line in the bottom panel of Figure 2 gives the parallel group velocity $V_{g\parallel} = \partial\omega/\partial k_\parallel$. This has a characteristic maximum at a relatively small value of $k_\parallel$, followed by a slow decrease to the asymptotic value for infinite $k_\parallel$, given by the dashed line. The properties in Figure 2 will be used later to interpret the numerical results obtained in the coupled case where k_y is small but not zero.

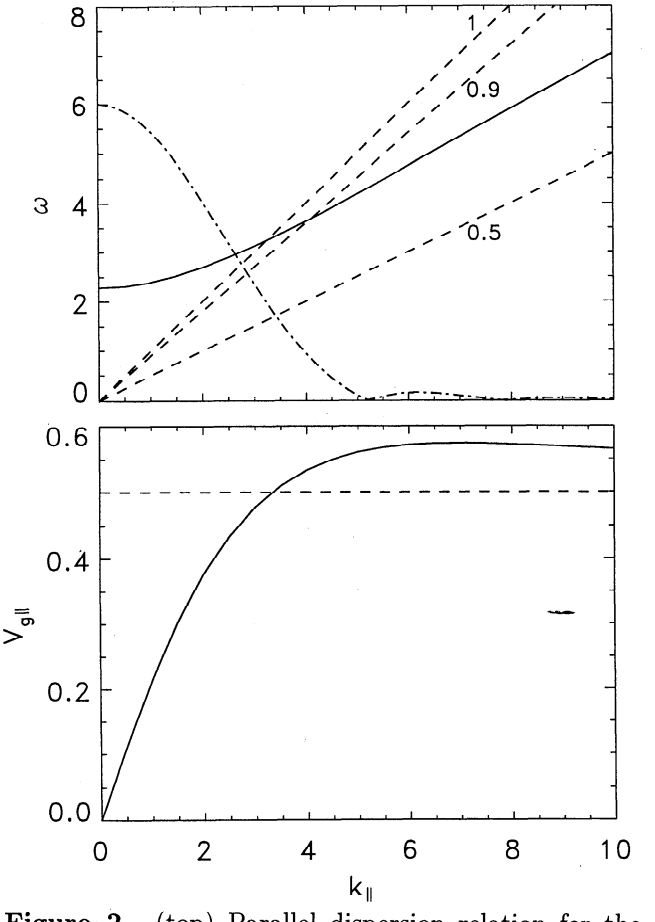

Figure 2. (top) Parallel dispersion relation for the $n = 1$ fundamental waveguide mode (solid line), the Alfvén wave dispersion relations for $V_A = 0.5$, 0.9, and 1 (dashed lines), and the initial perturbation $k_\parallel$ spectrum in arbitrary units (dash-dot line). (bottom) Parallel group velocity for the $n = 1$ waveguide mode (solid line) and the asymptotic value as $k_\parallel \to \infty$ (dashed line).

3. Numerical Solution

The system (3)–(7) is integrated forward in time using the leapfrog-trapezoidal algorithm [*Zalesak,* 1979] as described in section 3 of RW. This algorithm is second-order accurate in both space and time. Since the system is linear, we use a fixed time step equal to a fraction of the shortest Alfvén transit time across one cell of the grid. We use different (constant) grid spacings in x and z. A finer grid spacing is used in z as phase mixing in the z direction may ultimately develop some of the shortest spatial structures in the simulation. The grid spacing in x must be at least fine enough to resolve the x structure of the initial perturbation (8) well. In this perturbation of u_z we choose $t_d = 2$ and $x_d = 1.2$. Since wave propagation in the system is symmetrical about $z = 0$, we need solve only in the region $z \geq 0$ and then reflect the solution in the line $z = 0$ to obtain the complete solution.

We also choose $k_y = 0.5$ as the Fourier component perpendicular to the simulation plane allowing coupling between fast and Alfvén modes. If a half wavelength in y is taken as representing the width of the waveguide, then the width for $k_y = 0.5$ is 2π. This value of k_y ensures moderate coupling between fast and Alfvén modes, but larger values of k_y (and hence larger coupling) could be taken without making the waveguide unrealistically narrow. However, as discussed by RW, we wish to keep the coupling relatively weak so that energy densities derived using the field components of the uncoupled fast and Alfvén modes can still be used as approximate diagnostics for the propagation of the coupled modes.

Diagnostic checks were carried out using successively finer grid spacings until we were satisfied that the solutions had converged correctly. For example, when the driving condition (8) had unit amplitude, the difference between the u_z fields at the center of the $z > 0$ simulation box for a 100×500 grid and a 200×1000 grid in z and x was less than 5×10^{-3} when the code was run for 25 time units. In all runs we took the time step to be 1/20 of the shortest transit time between two adjacent grid points. The final configuration used had 200 grid points between $z = 0$ and 1. The length of the box x_E was chosen to be 25 in normalized units, and 1000 grid points were taken between $x = 0$ and x_E. The simulation was run for 25 time units so that disturbances traveling at the maximum Alfvén speed ($V_A = 1$) just reached the end of the box at $t = 25$. This ensures that the box acts as a true waveguide over the complete simulation time, with no interference from reflections at x_E. The grid spacing in z is small enough to ensure that the phase-mixing length (2) at $t = 25$ is well resolved.

For this configuration we found that the ratio of the wave energy in the box at $t = 25$ to the total injected energy was 0.9995. The maximum value of normalized $\nabla \cdot \mathbf{B}$ for all positions and times in the box was 10^{-12}. These figures convince us that the simulation is behaving properly.

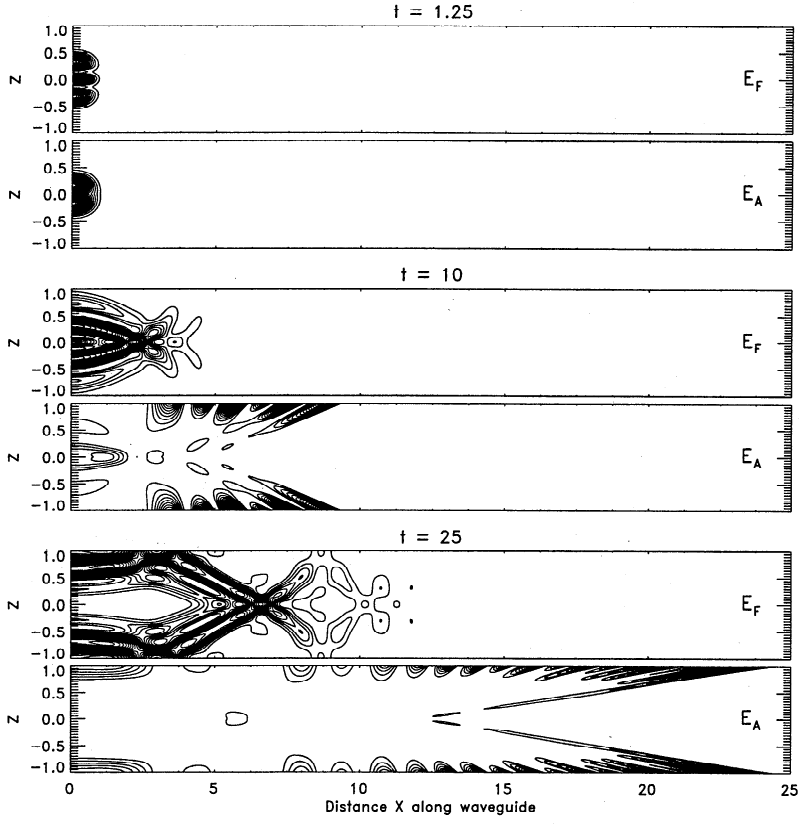

Figure 3. Contour plots of the fast mode energy density E_F and the Alfvén mode energy density E_A versus x and z for times $t = 1.25$, 10, and 25 during the simulation.

4. Results

As discussed earlier, we use energy densities derived from the field components of the uncoupled fast and Alfvén waves as approximate diagnostics of the relatively weakly coupled modes in the waveguide when k_y is not too large. The uncoupled ($k_y = 0$) fast and Alfvén mode energy densities E_F and E_A are given by

$$E_F = (\rho u_z^2 + b_x^2 + b_z^2)/2 \quad (9)$$

$$E_A = (\rho u_y^2 + b_y^2)/2 \quad (10)$$

We also use the diagnostic D_A defined by

$$D_A = u_y + b_y/\rho^{1/2} \quad (11)$$

which is exactly zero when the (u_y, b_y) wave field is purely Alfvénic. If the (u_y, b_y) perturbations are significantly non-Alfvénic, then D_A is nonzero.

In Figure 3 we display contour plots of E_F and E_A at times $t = 1.25$, 10, and 25 during the evolution of the simulation. Each contour plot is normalized to its own maximum value. Note how the development of the structure of E_F with time qualitatively resembles the development of the structure of the compressional magnetic field component shown in Figure 3 of *Wright* [1994]. Dispersion in the waveguide means that Fourier components with the largest $k_\parallel$ and smallest k_z propagate fastest down the waveguide, while components with smaller $k_\parallel$ and larger k_z propagate mainly across the waveguide, and travel much more slowly down the waveguide. At $t = 25$ in Figure 3, significant fast mode energy has only propagated about halfway down the waveguide. Most of the fast mode energy is still lingering near the beginning of the waveguide because the energy in the initial disturbance is mainly in small $k_\parallel$ components (see the dash-dot curve in the top panel of Figure 2).

The development of E_A in Figure 3 is of major interest. At $t = 1.25$ there is a clear E_A structure centered on the plasma sheet at $z = 0$ and associated with the developing E_F which initially was derived purely from u_z. At $t = 10$ new E_A structures have appeared near $z = \pm 1$. They originate at an x position within the propagating E_F structure but appear to have traveled down the waveguide at the local Alfvén speed for given z. This is confirmed at $t = 25$, where the origin of the E_A structures at $z = \pm 1$ is still associated with the slowly propagating E_F, but their leading edges at $z = \pm 1$ have almost reached the "earthward" end of the waveguide.

The E_A structures near $z = \pm 1$ appear to be Alfvénic in character. To test this we show in Figure 4 the field components u_y and b_y for $t = 1.25$, 10, and 25 at $z = 1$ and $z = 0.8$ along the complete waveguide. Also shown as dash-dot curves is the Alfvén diagnostic D_A given by (11). At $t = 1.25$ the initial disturbance has not yet reached $z = 1$, but a small non-Alfvénic disturbance

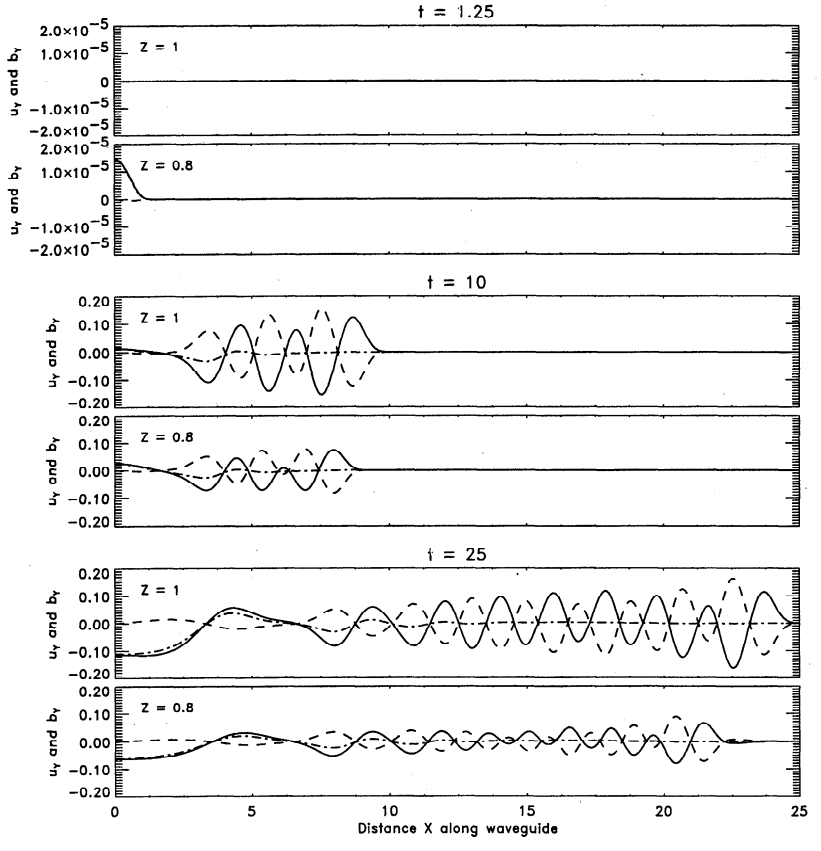

Figure 4. Velocity and magnetic field components u_y (solid lines) and b_y (dashed lines) versus x at $z = 1$ and 0.8 for times $t = 1.25$, 10, and 25. The Alfvén diagnostic D_A is shown by dash-dot lines.

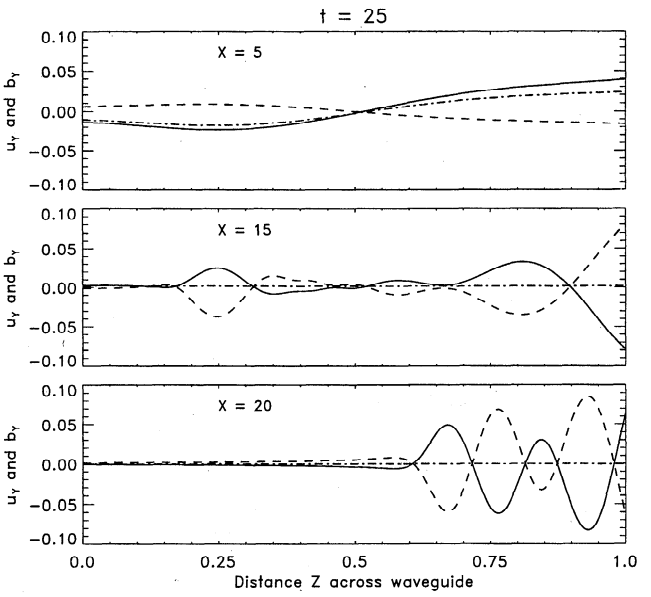

Figure 5. Velocity and magnetic field components u_y (solid lines) and b_y (dashed lines) versus z at $x = 5$, 15 and 20 for time $t = 25$. The Alfvén diagnostic D_A is shown by dash-dot lines.

has reached $z = 0.8$, with an extent in x comparable with (8). At $t = 10$ waves are propagating down the waveguide, becoming increasingly more Alfvénic as x increases. At $t = 25$, the structure at x less than about 7 is not Alfvénic, as D_A is definitely nonzero. For x greater than 7 the waves become more Alfvénic until by about $x = 14$ they appear to be virtually pure Alfvén waves. The wave at $z = 1$ is just reaching the end of the waveguide at $t = 25$, while the wave at $z = 0.8$ still has some way to go.

Figure 5 shows cuts of u_y and b_y across the northern lobe of the waveguide at $x = 5$, 15, and 20, for $t = 25$. The structure at $x = 5$ is not Alfvénic, while those at $x = 15$ and 20 are Alfvénic. At $x = 15$ the amplitude appears to decay inward from $z = 1$ to about $z = 0.5$, and then becomes enhanced again before becoming small near $z = 0$. At $x = 20$ there is a clear oscillatory structure for $z > 0.6$.

The general qualitative impression from these results is that part of the fast mode structure propagating relatively slowly down the waveguide is acting as a moving source of Alfvén waves near the $z = \pm 1$ boundaries of the waveguide. These Alfvén waves then propagate down the waveguide at the local Alfvén speed on a given field line. In the next section we consider more quantitative aspects of these ideas.

5. Discussion

5.1. Quantitative Interpretation

We begin by considering Alfvén waves that are not driven resonantly but are associated with the initial transient of the driving condition. These waves would exist on the field lines even if the $z = \pm 1$ boundaries were transparent to fast waves and no waveguide effects existed. Alfvén transients are seen most clearly in the E_A contour at $t = 25$ in Figure 3. Alfvén waves at $z = 0$ and ± 1.0 propagate at speeds of 0.5 and 1.0, respectively. Thus at $t = 25$ the transients have reached the points (x, z) of approximately (12.5, 0.0) and (25.0, ± 1.0). There is also a clear ridge of Alfvén energy joining these points associated with the transients on intermediate field lines. This leading edge delineates the propagating information front and the Alfvén waves that comprise it are not resonantly driven. The region to the right of the front is undisturbed by the driving condition. The Alfvén transient is also apparent in Figure 5: the profile at $x = 15$ (when $t = 25$) should reveal Alfvén waves propagating at a speed of 0.6, which corresponds to field lines at $z = 0.2$. Indeed, this z coordinate clearly identifies the leading Alfvén transient, although it occupies a range of z reflecting the fact that the driving source is extended in x and t. Similar reasoning suggests the profile at $x = 20$ (when $t = 25$) should have a transient feature propagating at a speed of 0.8 and be located around $z = 0.6$. The transient at $x = 20$ is adjacent to Alfvén waves ($z > 0.75$) that are resonantly driven, and we now focus upon these Alfvén waves.

The properties of the $k_y = 0$ uncoupled waveguide modes in Figure 2 can be used to interpret the small k_y coupled results described in the previous section. Significant coupling between fast waveguide modes and Alfvén modes (for a given $k_y \neq 0$) will occur when (1) the waveguide mode parallel phase velocity $V_{p\|}$ matches the Alfvén velocity and (2) there is significant power in the waveguide mode $k_\|$ spectrum at that phase velocity.

Coupling of fast and Alfvén waves can only occur when the fast frequency lies inside the Alfvén continuum. This corresponds to the solid line in the top panel of Figure 2 lying between the dashed lines labeled 0.5 and 1.0. When this condition is satisfied, the parallel phase velocity of the waveguide mode will match the Alfvén speed at some z value; this identifies the fieldline where "resonant" coupling can occur. The fast mode dispersion curve ($n = 1$) enters the Alfvén continuum at $(k_\|, \omega) = (3.3, 3.3)$, so fast modes with $k_\| < 3.3$ do not couple to Alfvén waves. The same panel also shows that the dominant power in the $k_\|$ spectrum is for $k_\|$ less than about 5. Hence significant mode coupling can only occur for waveguide modes with $3.3 < k_\| < 5.0$. The frequencies of these modes are in the range $3.3 < \omega < 4.2$, and the parallel phase velocities are $0.85 < V_{p\|} < 1.0$. Equating these phase velocities with Alfvén speeds identifies the layer of field lines on which Alfvén waves may be excited. Employing (1) implies the coupling layer is $0.7 < z < 1.0$. This is the case in Figures 3 and 5. At $x = 15$ in Figure 5 the lobe structure of the perturbation $k_\|$ amplitude spectrum in Figure 2 appears to be mirrored in the u_y and b_y amplitudes from about $z = 0.7$ to $z = 1.0$. At $x = 20$ a significant wave amplitude is also present between $0.6 < z < 0.7$ and is associated with the Alfvén transients discussed earlier in this subsection.

In the top panel of Figure 2 the intersections of the $V_A = 0.9$ and 1.0 lines (at $z = 0.8$ and 1.0) with the waveguide mode dispersion curve occur at $k_\parallel = 4.13$ and 3.30, respectively; these correspond to parallel wavelengths $\lambda_\parallel = 1.52$ and 1.91. From Figure 4 at $t = 25$ the measured wavelengths of the Alfvén waves over the interval for which the Alfvén diagnostic D_A is zero (after $x \approx 12$) are about 1.52 and 1.91 for $z = 0.8$ and 1.0, respectively. Therefore the Alfvén waves propagating in the model waveguide are consistent with generation by coupling to fast mode waves which approximately obey Figure 2.

The Alfvénic nature of the waves near $z = \pm 1$ was tested by plotting the position of the leading edge of the Alfvénic structure at $z = 1$ versus time. It was found to be moving at exactly unit speed, confirming it to be an Alfvén wave. At $z = 0.8$ the leading edge moves at the expected speed of 0.9 until about $t = 14$. After this time a small structure appears extending beyond the true leading edge (see the bottom panel of Figure 4). This structure has an amplitude of about 7×10^{-3}, comparable with the error discussed in section 3. We therefore interpret this as a numerical artifact which makes no difference to the qualitative insights gained in this paper. However, care would have to be taken to reduce the artifact for longer runs.

As discussed at the end of the previous section, the Alfvén waves at a given z appear to emanate from a source moving at a speed significantly less than $V_A(z)$. We have seen earlier that these Alfvén waves have $k_\parallel = 4.13$ and 3.30 at $z = 0.8$ and 1.0, respectively. The bottom panel of Figure 2 then gives the parallel group velocities of fast mode waves with these values of $k_\parallel$ as approximately $V_{g\parallel} = 0.55$ and 0.49, respectively. If we assume that fast mode wave packets moving at these values of $V_{g\parallel}$ are generating the Alfvén waves, then at $t = 25$ the source wave packets should have reached positions $x = 13.7$ and 12.4, respectively. These values are in excellent agreement with the positions in the bottom panel of Figure 4 which identify the points beyond which $D_A = 0$ (and the waves are Alfvénic) and before which D_A has a small but significant value (indicating the disturbance is not solely Alfvénic). We expect this as these positions should coincide with the leading edges of the driving fast wave packets. This supports our idea that the Alfvén waves at given z emanate continuously from a moving fast mode wave packet with parallel wavenumber at that z determined by the matching of phase speeds. The Alfvén waves then travel down the waveguide at speed $V_A(z)$. Note that the Alfvén wave energy is extracted from that part of the fast mode $k_\parallel$ spectrum which interacts with the Alfvén waves. Since the coupling was chosen to be small in this illustrative example, the Alfvén wave amplitudes are relatively constant on a given field line. If the coupling were chosen to be larger, the driving fast mode energy would be depleted, and we would expect to see the emitted Alfvén waves decrease in amplitude with time and z. Similar features would result if the fast mode energy leaked from the waveguide.

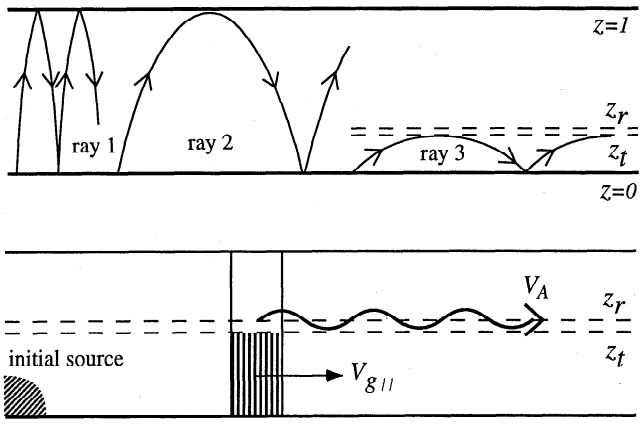

Figure 6. Schematic of ray trajectories and coupling site for the upper half of the magnetotail waveguide. (top) Three ray trajectories. Very low $k_\parallel$ waves are incident upon the "magnetopause" at $z = 1$ (ray 1). At larger $k_\parallel$ a critical value exists where the turning point is located at $z = 1$ (ray 2). For larger $k_\parallel$ the turning point (z_t) moves to lower Alfvén speeds. The mode couples resonantly to Alfvén waves at z_r which is located just beyond z_t. (bottom) A single $k_\parallel$ mode. It propagates away from the source region at speed $V_{g\parallel}$ and radiates an Alfvén wave at z_r which propagates with speed $V_A(z_r)$ ahead of the fast mode.

A cartoon of the fast waveguide mode propagation, dispersion and mode coupling to the Alfvén wave is shown in Figure 6. The top panel shows modes with a very small $k_\parallel$ which do not have a turning point inside $z = 1$ (ray 1). These waves are free to leak out unless the change in magnetoplasma parameters across $z = 1$ provides a sufficiently good reflecting boundary. As $k_\parallel$ is increased, trajectories like that of ray 2 are produced for which the turning point is located at $z = 1$. Increasing $k_\parallel$ still further moves the turning point deeper into the tail to smaller z (ray 3). In general, the turning point is located at z_t, defined via

$$\omega^2 = V_A^2(z_t)(k_y^2 + k_\parallel^2) \tag{12}$$

Since ω is a known function of $k_\parallel$ (Figure 2), the above equation effectively defines $k_\parallel(z_t)$ or equivalently $\omega(z_t)$. We expect small k_y modes to be most efficient at mode coupling to Alfvén waves as the resonant field line (at z_r) will be located near the turning point and will not require significant tunneling of fast mode energy. The location z_r is defined via

$$\omega^2 = V_A^2(z_r)k_\parallel^2 \tag{13}$$

so it is clear that for small k_y, $z_r \approx z_t$. Since ω is a known function of $k_\parallel$ (Figure 2), the above equation effectively defines $k_\parallel(z_r)$ or equivalently $\omega(z_r)$.

The lower panel in Figure 6 shows where the energy associated with fast modes in the interval $[k_\parallel, k_\parallel + dk_\parallel]$ is located. It moves along in a band at speed $V_{g\parallel}(k_\parallel)$ and has a width in x of $(\partial V_{g\parallel}/\partial k_\parallel)dk_\parallel t$, where t is the

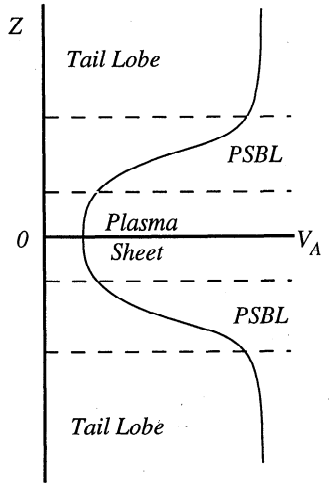

Figure 7. Schematic of a possible Alfvén speed structure within the plasma sheet, plasma sheet boundary layer (PSBL), and tail lobe.

time since the waves were excited. The width broadens in time due to dispersion. The energy is concentrated on the low Alfvén speed side of the turning point. While the band of fast mode energy is propagating along the guide, it is also coupling to Alfvén waves at z_r which are radiated from the moving source and propagate at a speed $V_A(z_r)$. Thus the Alfvén waves run ahead of the fast mode source region.

Figure 6 illustrates that the efficiency of the boundary at $z = 1$ as a reflector is not an important factor in containing the critical part of the fast mode energy spectrum in the waveguide. Rays which do not have a turning point before $z = 1$ may be lost through the boundary if it is not a good reflector. Rays which interact with Alfvén waves have turning points inside the waveguide and are evanescent for $z > z_t$. Such modes do not lose significant energy through the $z = 1$ boundary and are fairly insensitive to the boundary condition imposed there.

In Figure 7 we sketch a probable region where the ideas described in this paper could apply. The Alfvén speed in the plasma sheet and the plasma sheet boundary layer (PSBL) varies with z roughly as shown in Figure 7 before the more constant conditions of the tail lobe are reached. We expect that Alfvén waves generated by guided fast mode waves are most likely to exist in the PSBL.

5.2. Phase-Mixing Lengths

The Alfvén waves running ahead of the fast source regions are essentially decoupled Alfvén waves which will phase mix and produce small scale lengths in the z direction. (This can be seen in the bottom panel of Figure 5.) Previous studies of phase mixing have either looked at time dependent systems in which the (Alfvén) frequency of each field line is a function of position but $k_\parallel$ is constant [e.g., *Mann et al.*, 1995], or considered normal modes in which $k_\parallel$ is a function of position, but ω is constant [e.g., *Heyvaerts and Priest*, 1983]. The situation in our present study includes the richness of both types of phase mixing: we noted above that (13) defines $k_\parallel$ and ω_A for Alfvén waves that will be excited resonantly at a given z.

Energy has propagated away from the region around $(0, 0)$ since $t = 0$. Subsequent propagation would suggest a local mode structure of $\exp i\phi$,

$$\phi = k_\parallel(z)\, x - \omega_A(z)\, t \tag{14}$$

where $k_\parallel(z)$ is the parallel wave number for which fast and Alfvén waves are resonant at z, and $\omega_A(z)$ is the frequency of these waves. The local phase mixing length in z of this solution is $L_{PH} = 2\pi/k_z(z)$, where

$$k_z \approx \frac{\partial \phi}{\partial z} = k'_\parallel\, x - \omega'_A\, t \tag{15}$$

and a prime denotes $\partial/\partial z$.

Since we have already quoted the values of V_A and $k_\parallel$ at $z = 0.8$ and 1.0, it is easy to estimate the gradients of ω_A and $k_\parallel$ at $z = 0.9$, and thus the phase-mixing length there. These gradients are $k'_\parallel(z = 0.9) \approx -4.20$, and $\omega'_A(z = 0.9) \approx -2.15$. The bottom panel of Figure 5 enables us to measure the phase-mixing length at $z = 0.9$ from the numerical solution to be about 0.2. These waves are observed at $t = 25.0$, $x = 20.0$ from which we can estimate the phase-mixing length to be 0.208, which is in excellent agreement with the value measured from Figure 5. It is interesting to note that the phase mixing from gradients in $k_\parallel$ and ω_A tend to cancel each other, and it is important to include both mechanisms. If we only include one or the other process we get the following estimates for the phase-mixing length, $2\pi/(\omega'_A t) = 0.117$, and $2\pi/(k'_\parallel x) = 0.075$, neither of which is close to the measured value. Since the two contributions to the phase mixing tend to cancel each other out (i.e., reduce k_z in (15)), the system takes longer to develop small scales than the less sophisticated estimate in (2) suggests. This is important for deciding whether electron inertial or finite Larmor radius effects will become significant.

5.3. Application to the Magnetosphere

Our model magnetosphere is very idealized and does not include several features of the physical magnetosphere, for example, variation of parameters in the x direction. Flaring of the tail results in an increase in cross-sectional area and a decrease in the lobe magnetic field with antisunward distance. However, flaring becomes very gradual beyond about 20–30 R_E downtail of the Earth [*Petrinec and Russell*, 1996]. Over most of the region in which fast waveguide modes couple to Alfvén waves the structure should be reasonably independent of x. Only in the near-Earth region is there a significant change in the waveguide parameters. This may affect some long-wavelength components of the dispersive fast mode structure but should have no significant effect on the field-guided Alfvén waves. We feel that the following results should apply at least qualitatively to the physical magnetosphere.

1. A significant energy release in the far tail plasma

sheet should result in the launching of fast waveguide modes toward and away from the Earth.

2. If the energy release has a reasonable extent along the waveguide (of the order of the lobe width), most of the fast mode energy will travel relatively slowly toward the Earth because of the slow parallel group velocities of the waveguide modes with significant energy. Very small $k_{||}$ modes that do not have a turning point inside the magnetopause may escape to the magnetosheath.

3. A range of these fast waveguide modes can couple with Alfvén waves in a limited region containing field lines on which the parallel phase velocities of the fast and Alfvén modes match. These waveguide modes act as moving sources emitting Alfvén waves ahead of the fast mode.

4. The excited Alfvén waves travel in front of the fast modes (on any given field line) at the local Alfvén speed, which is generally significantly larger than the source speeds (i.e., $V_{g||}$).

5. Similar waveguide modes may be launched antisunward down the tail and drive antisunward propagating Alfvén waves.

6. Our model does not have a single resonant field line but a layer of field lines on which Alfvén waves are resonantly driven. The width of the layer can be determined from the equilibrium structure of the waveguide and the parallel extent of the source region.

Point 4 means that pure Alfvén waves should arrive at the Earth well before fast mode waves with comparable energy. Fast waves may lose significant energy through the flanks of a realistic model, and so we anticipate that not all of the fast mode energy will reach the near-Earth magnetosphere. Also field lines at high magnetic latitudes become distorted as they approach the Earth. Alfvén waves should be guided to the high-latitude ionosphere along these field lines, but fast mode energy may be lost across the field lines before reaching the ionosphere. The wave signature at the high-latitude ionosphere may therefore be predominantly Alfvénic. If we choose $z_M = 20\,R_E$ and $V_{AM} = 700\ \mathrm{km\,s^{-1}}$, the model time unit is 180 s. Alfvén wave frequencies near $z = \pm 1$ are then about 3 mHz, similar to frequencies observed under the ionosphere in the region where field lines are extremely stretched or open [*Ables et al.*, 1996; *Wolfe et al.*, 1997a, b].

A further interesting effect of point 4 is that the Alfvén waves "phase mix" as they travel toward the Earth at different speeds on adjacent field lines [e.g., *Heyvaerts and Priest*, 1983; *Nocera et al.*, 1984; *Mann et al.*, 1995]. Our results generalize these studies by including both spatial and temporal phase mixing. This generates increasingly finer transverse spatial scales as the waves propagate, an effect which can be clearly seen in Figure 5. If fine enough scales can develop (because of long propagation distances, steep Alfvén speed gradients, or both), it is possible that nonhydromagnetic effects may occur. For example, if the transverse scale length approaches the ion Larmor radius, the Alfvén waves may begin to disperse across the field lines [e.g., *Streltsov and Lotko*, 1995]. Similar effects would occur if the transverse scale length approaches the electron inertia length. To estimate these parameters, we take $B_0 \sim 10$ nT, an ion temperature of 10^7 K, and an electron number density of $5 \times 10^5\ \mathrm{m^{-3}}$ [*Paterson and Frank*, 1994]. These give an ion Larmor radius of about 300 km, and an electron inertia length of about 10 km. With $z_M = 20\,R_E$ our phase mixing length of 0.2 becomes $4\,R_E$. It therefore seems likely that two-fluid effects will still be insignificant by the time our Alfvén waves reach the Earth. Of course, the equilibrium structure of the tail will determine the details of how rapidly phase mixing will occur. Our equilibrium was chosen for numerical convenience. The use of a more realistic model where localized large density gradients may occur will alter the phase mixing length estimates.

Note that our normalized waveguide length of 25 means that our perturbation occurs in the far tail. It is uncertain how far down-tail such disturbances can occur. However, our intention here has been to give enough propagation time to allow the obvious development of features such as phase mixing.

6. Conclusions

We have presented a numerical simulation of hydromagnetic wave propagation in a simplified magnetospheric tail, modeled as a hydromagnetic waveguide with uniform longitudinal magnetic field and a transverse density gradient chosen to give an Alfvén speed which increases linearly across each lobe from the thin "plasma sheet" to the nominal "magnetopause."

A relatively short (in duration and longitudinal extent) transverse velocity perturbation is applied at the far tail end of the waveguide's plasma sheet. This propagates dispersively down the waveguide in the form of fast waveguide modes. Fourier components with small parallel wavenumber contain most of the energy and propagate relatively slowly toward the "Earth." Components above a critical $k_{||}$ act as moving sources which launch Alfvén waves continuously earthward. The wave dispersion relations are such that the waveguide modes couple with Alfvén waves only in a limited region of the transverse Alfvén speed gradient. The Alfvén waves travel at the local Alfvén speed along each field line, so that as they travel the wave on a given field line becomes increasingly out of phase with waves on adjacent field lines. This phase-mixing process leads to increasingly fine transverse structure as the waves progress down the waveguide, but the structure is not likely to become fine enough to allow two-fluid effects to develop unless the local Alfvén speed gradients are very steep.

We conclude that energy releases in the far tail which result in a transverse displacement of the tail field lines should have signatures which propagate up- and down-tail from the source region as relatively slowly moving compressional waveguide modes. In a limited region of any transverse Alfvén speed gradient these modes should launch Alfvén waves which propagate ahead of the fast wave front. The latter should be seen in and below the high-latitude ionosphere as a train of Alfvén waves of significant duration on stretched or open field

lines. This could possibly be followed by compressional wave signatures if the waveguide modes reach the high-latitude ionosphere with significant amplitudes. Note that this mechanism provides a way of generating oscillatory Alfvén wave signatures without requiring standing waves on closed field lines and should be applicable in regions such as the plasma sheet boundary layer and the plasma mantle.

Acknowledgments. We thank the referees for very useful comments which have improved this paper. W.A. acknowledges support by the New Zealand Foundation for Research, Science and Technology (FRST) through contract CO1627. A.N.W. is supported through a U.K. PPARC Advanced Fellowship and is gratcful to PPARC and FRST for funding his visit to NIWA, New Zealand.

The Editor thanks M. J. Engebretson and another referee for their assistance in evaluating this paper.

References

Ables, S. T., B. J. Fraser, H. J. Hansen, F. W. Menk, and R. J. Morris, Polarisation characteristics of long period geomagnetic pulsations recorded at Antarctic stations, *ANARE Res. Notes 95*, pp. 112–124, Aust. Natl. Antarct. Res. Exped., Aust. Antarct. Div., Melbourne, Victoria, 1996.

Berghmans, D., P. De Bruyne, and M. Goossens, The footpoint driven coronal sausage wave, *Astrophys. J., 472,* 398–411, 1996.

Edwin, P. M., B. Roberts, and W. J. Hughes, Dispersive ducting of MHD waves in the plasma sheet: A source of Pi2 wave bursts, *Geophys. Res. Lett., 13,* 373–376, 1986.

Elphinstone, R. D., et al., The double oval UV auroral distribution, 2, The most poleward arc system and the dynamics of the magnetotail, *J. Geophys. Res., 100,* 12,093–12,102, 1995.

Herron, T. J., An average geomagnetic power spectrum for the period range 4.5 to 12,900 seconds, *J. Geophys. Res., 72,* 759–761, 1967.

Heyvaerts, J., and E. R. Priest, Coronal heating by phase-mixed shear Alfvén waves, *Astron. Astrophys., 117,* 220–234, 1983.

Hopcraft, K. I., and P. R. Smith, Magnetohydrodynamic waves in a neutral sheet, *Planet. Space Sci., 34,* 1253–1257, 1986.

Liu, W. W., B.-L. Xu, J. C. Samson, and G. Rostoker, Theory and observation of auroral substorms: A magnetohydrodynamic approach, *J. Geophys. Res., 100,* 79–85, 1995.

Mann, I. R., A. N. Wright, and P. S. Cally, Coupling of magnetospheric cavity modes to field line resonances: A study of resonance widths, *J. Geophys. Res., 100,* 19,441–19,456, 1995.

McClay, J. R., and H. R. Radoski, Hydromagnetic propagation in a theta-model geomagnetic tail, *J. Geophys. Res., 72,* 4525–4528, 1967.

McKenzie, J. F., Hydromagnetic oscillations of the geomagnetic tail and plasma sheet, *J. Geophys. Res., 75,* 5331–5339, 1970.

McKenzie, J. F., Hydromagnetic wave coupling between the solar wind and the plasma sheet, *J. Geophys. Res., 76,* 2958–2966, 1971.

Nocera, L., B. Leroy, and E. R. Priest, Phase mixing of propagating Alfvén waves, *Astron. Astrophys., 133,* 387–394, 1984.

Patel, V. L., Magnetospheric tail as a hydromagnetic wave guide, *Phys. Lett., 26A,* 596–597, 1968.

Paterson, W. R., and L. A. Frank, Survey of plasma parameters in Earth's distant magnetotail with the Geotail spacecraft, *Geophys. Res. Lett., 21,* 2971–2974, 1994.

Petrinec, S. M., and C. T. Russell, Near-Earth magnetotail shape and size as determined from the magnetopause flaring angle, *J. Geophys. Res., 101,* 137–152, 1996.

Radoski, H. R., A note on the problem of hydromagnetic resonances in the magnetosphere, *Planet. Space Sci., 19,* 1012–1013, 1971.

Rickard, G. J., and A. N. Wright, Alfvén resonance excitation and fast wave propagation in magnetospheric waveguides, *J. Geophys. Res., 99,* 13,455–13,464, 1994.

Rickard, G. J., and A. N. Wright, ULF pulsations in a magnetospheric waveguide: Comparison of real and simulated satellite data, *J. Geophys. Res., 100,* 3531–3537, 1995.

Roberts, B., P. M. Edwin, and A. O. Benz, On coronal oscillations, *Astrophys. J., 279,* 857–865, 1984.

Samson, J. C., B. G. Harrold, J. M. Ruohoniemi, R. A. Greenwald, and A. D. M. Walker, Field line resonances associated with MHD waveguides in the magnetosphere, *Geophys. Res. Lett., 19,* 441–444, 1992.

Seboldt, W., Nonlocal analysis of low-frequency waves in the plasma sheet, *J. Geophys. Res., 95,* 10,471–10,479, 1990.

Siscoe, G. L., Resonant compressional waves in the geomagnetic tail, *J. Geophys. Res., 74,* 6482–6486, 1969.

Southwood, D. J., Some features of field line resonances in the magnetosphere, *Planet. Space Sci., 22,* 483–491, 1974.

Streltsov, A., and W. Lotko, Dispersive field line resonances on auroral field lines, *J. Geophys. Res., 100,* 19,457–19,472, 1995.

Walker, A. D. M., J. M. Ruohoniemi, K. B. Baker, R. A. Greenwald, and J. C. Samson, Spatial and temporal behavior of ULF pulsations observed by the Goose Bay HF radar, *J. Geophys. Res., 97,* 12,187–12,202, 1992.

Walker, A. D. M., J. M. Ruohoniemi, K. B. Baker, R. A. Greenwald, and J. C. Samson, Spectral properties of magnetotail oscillations as a source of Pc5 pulsations, *Adv. Space Res., 13,* (4)59–(4)65, 1993.

Weatherwax, A. T., T. J. Rosenberg, C. G. Maclennan, and J. H. Doolittle, Substorm precipitation in the polar cap and associated Pc 5 modulation, *Geophys. Res. Lett., 24,* 579–582, 1997.

Wolfe, A., L. J. Lanzerotti, C. G. Maclennan, and A. T. Weatherwax, ULF waves on open field lines (abstract), *Eos Trans. AGU, 78(17),* Spring Meet. Suppl., S227, 1997a.

Wolfe, A., L. J. Lanzerotti, C. G. Maclennan, and A. T. Weatherwax, Large amplitude hydromagnetic waves on open geomagnetic field lines, *Antarct. J. U. S.*, in press, 1997b.

Wright, A. N., Dispersion and wave coupling in inhomogeneous MHD waveguides, *J. Geophys. Res., 99,* 159–167, 1994.

Wright, A. N., and G. J. Rickard, ULF pulsations driven by magnetopause motions: Azimuthal phase characteristics, *J. Geophys. Res., 100,* 23,703–23,710, 1995.

Zalesak, S. T., Fully multidimensional flux-corrected transport algorithms for fluids, *J. Comput. Phys., 31,* 335–362, 1979.

W. Allan, National Institute of Water and Atmospheric Research, P. O. Box 14-901, Kilbirnie, Wellington, New Zealand. (e-mail: w.allan@niwa.cri.nz)

A. N. Wright, Mathematical Institute, University of St. Andrews, Fife KY16 9SS, Scotland.
(e-mail: andy@dcs.st-and.ac.uk)

(Received June 11, 1997; revised September 15, 1997; accepted October 8, 1997.)